

A new scheme for isomer pumping and depletion with high-power lasers

C.-J. Yang,¹ K. M. Spohr,^{1,2} M. Cernaianu,¹ D. Doria,¹ P. Ghenuche,¹ and V. Horný¹

¹*ELI-NP, “Horia Hulubei” National Institute for Physics and Nuclear Engineering,
30 Reactorului Street, RO-077125, Bucharest-Magurele, Romania**

²*School of Computing, Engineering and Physical Sciences,
University of the West of Scotland, High Street, PA1 2BE, Paisley, Scotland†*

(Dated: July 25, 2025)

We propose a novel scheme for the population and depletion of nuclear isomers. The scheme combines the γ -photons with energies $\gtrsim 10$ keV emitted during the interaction of a contemporary high-intensity laser pulse with a plasma and one or multiple photon beams supplied by intense lasers. Due to nonlinear effects, two- or multi-photon absorption dominates over the conventional multi-step one-photon process for an optimized gamma flash. Moreover, this nonlinear effect can be greatly enhanced with the help of externally supplied low-energy photons coming from another laser. These low-energy photons act such that the effective cross-section experienced by the γ -photons becomes tunable, growing with the intensity I_0 of the beam. Assuming $I_0 \sim 10^{18}$ Wcm⁻² for the photon beam, an effective cross-section as large as 10^{-21} cm² to 10^{-28} cm² for the γ -photon can be achieved. Thus, within state-of-the-art 10PW laser facilities, the yields from two-photon absorption can reach 10^6 to 10^9 isomers per shot for selected states that are separated from their ground state by E2 transitions. Similar yields for transitions with higher multiplicities can be accommodated by multi-photon absorption with additional photons provided.

PACS numbers: 25.30.Bf, 21.60.Cs, 01.30.-y, 01.30.Ww, 01.30.Xx

I. INTRODUCTION

Nuclear isomers are excited states of nuclei that have a longer half-life ($t_{1/2} \gtrsim 1$ ns) than the states in the prompt decay paths of a nucleus following an induced excitation. Isomers with $t_{1/2} > 10$ years (e.g., ^{93m}Nb, ^{113m}Cd, ^{178m}Hf, etc.) are ideal candidates for nuclear batteries that outperform conventional ones by $\times 10^6$ in energy density [1]. Many isomers with $t_{1/2} \gtrsim$ hours have proven medical potentials [2–4]. Furthermore, isomers generally serve as pathways to enable nuclear lasing [5, 6]. Since their discovery [7], the efficient creation and induced depopulation of isomers has been one of the outstanding problems in physics. Any breakthrough on this topic will enable exciting applications in nuclear photonics.

The production of isomers by brute force via photon absorption toward the desired state is inefficient and riddled with technological challenges. In general, it requires pumping through intermediate states with shorter lifetimes, except for a few cases where favorable transitions of ground-state to a higher excited state followed by its decay into the isomer state exist. Herein, the dilemma is that generating a large number of γ -photons to be absorbed resonantly by the nuclear level within a short time is difficult. Moreover, the direct pumping of a state exhibiting a longer half-life is challenged by the relatively narrow absorption bandwidth (e.g., 10 ps correspond to a natural width of only $6.6 \cdot 10^{-5}$ eV), which leads to the so-called graser dilemma, i.e., the half-life/width combinations given in nature require elusive laser pumping

powers or the very unrealistic scenario of an induced nuclear explosion [5, 6]. As the energy gap between nuclear transitions often leads to isomers $\gtrsim 100$ keV, no existing laser can be used in direct pumping, with a few exceptions such as, e.g., ²²⁹Th [8, 9].

Other than γ -excitation, alternative ways of generating isomers discussed in the past involve various nuclear reactions or Coulomb excitation, provided that suitable seed nuclei are available [10, 11]. However, triggered depletion of isomers, ie, how to harvest energy with high efficiency, seems still an unsolvable problem [8, 12–33]. Nevertheless, proposals that utilizing intensive ($\gtrsim 10^{10}$ Wcm⁻²) optical photons toward a virtual state followed by spontaneous emissions to the desired state provide an interesting alternative [34–37].

High-power laser systems (HPLS) can become core entities to spearhead associated developments [38–50] as they are now able to deliver intensities up to $\mathcal{P} \sim 10^{21-23}$ Wcm⁻² [51–56] (see <https://www.icuil.org/> for a comprehensive overview of current facilities). When interacting with an overdense target, HPLS accelerate electrons in the materials to highly relativistic energies and drive strong currents in the plasma environment. The extreme, quasistatic magnetic fields then interact with energetic electrons, generate dense γ -photons [57–68] and rejuvenates the hope of a mass production of isomers. However, existing schemes of manipulating isomers incorporate single- or multi-step excitation via very dense γ -photons to some “stepping” intermediate states in the decay chain toward the desired state [29, 30, 69, 70], which, even with an optimal HPLS-based γ -production, give yield estimates that are far from even suggesting a technical realization [67, 71–79]. Reaching a sufficient population yield for the isomer population remains an

* chieh.jen@eli-np.ro (corresponding author)

† klaus.spohr@eli-np.ro (corresponding author)

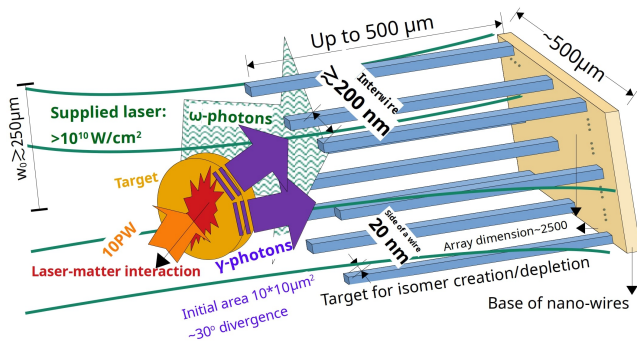


Figure 1. Schematic illustration of the proposed scheme with a possible target design. Note that the two-directional γ -photons corresponds to the laser-matter interaction scheme which has the most intense γ -flux in Fig. 2, while in general the γ -photons can have varied characteristics. (Dimensions not to scale, see supplemental materials for reasons behind the given parameters)

insurmountable challenge.

In this work, we demonstrate that the efficiency of isomer pumping and successive depletion can be drastically improved ($\geq 10^{10}$ -fold) by combining the γ -photons generated by an HPLS with intense supplied optical/infrared photons ($\equiv \omega$ -photons), through a two- or multi-photon absorption (nPA) mechanism, as illustrated in Fig. 1. This nPA mechanism prescribes a non-linear growth of yields [34–36, 80–83] and becomes dominant as the intensity of the incident photons increases.

II. THEORY

Denoting E_i and I_i the energy and the corresponding intensity (note that I_i is the number of photons per area per time, while $\mathcal{P}_i \equiv I_i E_i$ is the energy flux—which is later denoted as intensity in the unit of Wcm^{-2}) of the i^{th} photon category in an nPA process. Assuming the energies are tunable so that $E \equiv \sum_{i=1}^n E_i$ equals the gap between the initial state and the state one wishes to populate, then

$$\frac{d\mathcal{Y}_{(n)}}{dz} = N \cdot (I_1 I_2 \cdot \dots \cdot I_n \sigma_{npa} + \dots), \quad (1)$$

where $\mathcal{Y}_{(n)}$ denotes the yields of the final state per unit time given by n -photon absorption, N is the number of nuclei photons encountered per distance in the target dz , and σ_{npa} is the generalized cross-section for nPA and is a function of each E_i . The unit of σ_{npa} is $[\text{length}]^{2n}[\text{time}]^{n-1}$, i.e., a direct extension to the well-known 2PA cross-section ($\sigma_{2pa} = \sigma_{GM}$)[80]. Note that nPA corresponds to iterations on the interaction Hamiltonian H_{int} —which is normally further expanded into electromagnetic multipoles. Therefore, unless the product of intensities reaches a sufficient threshold, $I_1 I_2 \cdot \dots \cdot I_n \sigma_{npa}$ is negligible compared to 1PA with an H_{int} equal

to the multipolarities of the transition. Conversely, additional terms (denoted as “...” in Eq. (1)) will dominate over $I_1 I_2 \cdot \dots \cdot I_n \sigma_{npa}$ if any of the I_i satisfies

$$\sigma_{npa} < I_i \sigma_{(n+1)pa}. \quad (2)$$

In this case, two photons (instead of one) in the i^{th} category being absorbed at once will be preferred, and the original nPA process is surpassed by a $(n+1)$ PA process. The fundamental reason for this enhancement lies in combinatorial enhancement as illustrated in Fig. 1 of Ref. [84], which makes multiphoton absorption more efficient than single-photon absorption under an intense environment. One can rewrite $I_1 I_2 \sigma_{2pa}$ as $I_1 \sigma_{eff}(I_2)$ for 2PA. Thus, the effective cross-section $\sigma_{eff}(I_2)$ experienced by those I_1 -photons becomes tunable and depends on I_2 . The dependence is linear only when I_2 is low, i.e., $\sigma_{eff}(I_2) \sim I_2 \sigma_{2pa}$, but becomes $\sim I_2^2 \sigma_{3pa}$ when I_2 reaches a critical value so that $\sigma_{2pa} < I_2 \sigma_{3pa}$. For convenience, we assume that all of the I_i in Eq. (1) are below their critical values governed by Eq. (2). Any exceeding I_i will be re-distributed in favor of a new category $(n+1)$, as $(n+1)$ PA dominates in this case. In that case, one can define the effective cross-section experienced by I_1 (via nPA) as

$$\sigma_{eff}^{npa}(I_2, I_3, \dots, I_n) = I_2 \cdot \dots \cdot I_n \sigma_{npa}, \quad (3)$$

where the unit of σ_{eff}^{npa} is $[\text{length}^2]$. The remaining task is to estimate the size of σ_{npa} . The concept of nPA has been widely practised in atomic and molecular physics, though it has yet to be observed experimentally in nuclear systems. Only reverse processes have been observed based on double γ -decay [85–93]. Nevertheless, the theoretical derivation first introduced by Göppert-Mayer [80] and its later extensions [94–96] are very general and do not rely on whether the systems at hand are nuclei or atoms. Denoting e as the charge, $|i\rangle$, $|m\rangle$ and $|f\rangle$ as the initial, intermediate, and final state in the process, the transition rate of 2PA reads [97],

$$R_{2pa} = \frac{e^4 \mathcal{E}_1^2 \mathcal{E}_2^2}{16\hbar^4} |\mathcal{M}|^2 2\pi \delta_t(\omega - \omega_1 - \omega_2), \quad (4)$$

where $\omega_i = E_i/\hbar$, with E_i the energy of the i^{th} -category photons with amplitude \mathcal{E}_i , \hbar the reduced Planck constant. δ_t has the dimension of [time], and

$$\mathcal{M} = \sum_m \left[\frac{\langle f | \hat{H}_2 | m \rangle \langle m | \hat{H}_1 | i \rangle}{\omega_1 - \omega_{mi}} + (1 \leftrightarrow 2) \right], \quad (5)$$

where $\omega_{mi} = \omega_m - \omega_i$ is the energy gap between the initial and the m state, with m representing a physical state which belongs to any eigenstate of the nuclear Hamiltonian (including i or f itself). To maximize the transition amplitude $|\mathcal{M}|$, the virtual state after each photon absorption needs to resonate with a physical state to minimize the denominators of Eq. (18).

In the atomic case, the wavefunctions of excited-states can be calculated accurately [98–102], which enables an

evaluation of $|\mathcal{M}|$ [95, 96, 103–109]. Unfortunately, most excited states of nuclei cannot be accurately described due to a combination of a complicated structure of nuclear forces and the difficulty of solving the nuclear many-body problem [110–113]. In this work, we do not focus on specific nuclei and adopt the Weisskopf estimates [114] to evaluate the transition operators $\langle \hat{H}_i \rangle$ due to the i^{th} photon. For convenience, we define $i = 1$ as the γ -photons and $i = 2$ as the ω -photons.

We consider two cases for 2PA. Case (a) represents the situation that no intermediate state within ~ 1 keV from $\langle i |$ or $\langle f |$ exists. Therefore, the virtual state needs to resonate with either $\langle i |$ or $\langle f |$ itself, causing the denominator in Eq. (18) to become ω_2 (i.e., the one labeled as the supplied photon). The corresponding transition \hat{H}_2 must be at least M1 or higher, as $\langle m |$ is represented by either $\langle i |$ or $\langle f |$ and the angular momentum quantum number between the transition $\Delta J^\pi = 0^+$. Furthermore, one needs to exclude the transition from $J = 0$ to $J = 0$, which is forbidden for a single photon in the first order [85]. For \hat{H}_1 , E1 gives the largest possible matrix element. Case (b) has $\langle m |$ separated from $\langle i |$ or $\langle f |$ by $\Delta J^\pi = 1^-$ and $\Delta E \lesssim 1$ keV. In this case, each photon can undergo E1 transition.

The difference between case (a) and (b) is whether the ω -photons perform M1 or E1 transitions. As the typical ratio of transition probabilities between E1 and M1 ranges from $10^1 - 10^3$, case (b) will become negligible compared to (a) if the aforementioned gap $\Delta E > 1$ keV, due to a larger denominator in Eq. (18).

We note that $\langle i |$ and $\langle f |$ can be any eigenstate of the nuclear Hamiltonian. For isomer creation, $\langle f |$ is the isomer or a higher excited state that has a favorable decay path to the desired isomer, and $\langle i |$ is the initial state. For depletion, $\langle i |$ is the isomer and $\langle f |$ is the state one wishes to arrive, which can be any excited state with J^π favorable for decaying into the ground-state.

III. YIELDS ESTIMATE

The realistic cross-section of 2PA is conventionally expressed as [105]

$$\sigma_{2pa} = \sigma_0 g G, \quad (6)$$

with σ_0 (unit: $[\text{length}]^4$) the line-shape-independent cross-section, g (unit: $[\text{time}]$) the line-shape function, and G the photon statistical factor [115, 116]. $G = 1$ for a single-mode laser and becomes larger in multi-mode cases. The value of g can be estimated by a Gaussian distribution with a full width at half maximum (FWHM) equal to the greater of the width ($\equiv w_>$) of $\langle f |$ or the laser bandwidth.

$$g = 2\sqrt{\frac{\ln 2}{\pi}} \frac{1}{w_>} \sim \frac{0.939}{w_>}. \quad (7)$$

One can see that σ_{2pa} is weakened by $w_>$, which is dominated by recoil broadening and should not exceed 1 eV

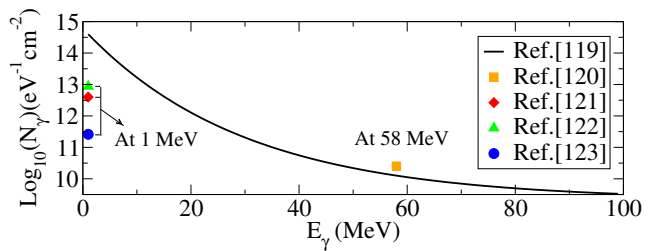


Figure 2. Number of γ -photons N_γ per eV cm^2 as a function of energy generated via laser-plasma interaction in a single shot converted from Refs. [119–123], with details listed in supplemental material [97]. Note that the actual γ -flux occupies an area of only $\approx 100 \mu\text{m}^2$. The accumulated time is $t \approx 15 - 50$ fs.

for solid targets. Using ultra-intense beams could potentially broaden $w_>$ [117] and free the nuclei in the solid target for an intensity $\gtrsim 10^{18} \text{ Wcm}^{-2}$.

With detailed derivations given in the supplemental materials [97], the effective cross-section (given in $[\text{cm}^2]$) experienced by the γ -photon reads

$$\sigma_{eff}^{2pa, E1+E1} \approx 3 \cdot 10^{-51} \frac{E_\gamma}{w_>} \mathcal{P}_2 \frac{A^{4/3}}{(\Delta E)^2} G, \quad (8)$$

$$\sigma_{eff}^{2pa, M1+E1} \approx 5 \cdot 10^{-51} \frac{E_\gamma}{w_>} \mathcal{P}_2 \frac{A^{2/3}}{(E_2)^2} G, \quad (9)$$

where the superscripts $M1 + E1$ and $E1 + E1$ represent cases (a) and (b), respectively. E_γ and $w_>$ must have the same unit, \mathcal{P}_2 is the intensity of the supplied laser in Wcm^{-2} , $\Delta E = |E_m - E_{i/f}|$ (in eV) is the gap between $\langle m |$ and the nearest of the initial/final state, which reduces to E_2 in the case of $M1 + E1$. A is the number of nucleons.

Eq. (8) and (9) agree with the estimates in Refs. [35, 82] if one adopts $G = 1$ and the natural width of $\langle f |$ for $w_>$. However, this is likely to apply only in the cases of Mößbauer nuclei [118]. In general, $w_>$ is likely to be $10^3 \sim 10^4$ times larger. Thus, the effective cross-section (10^{-26} cm^2 to 10^{-32} cm^2 for $A \approx 200$ nuclei) given before by assuming $\mathcal{P}_2 = 10^{10} \text{ Wcm}^{-2}$ will be suppressed accordingly. However, today's lasers can reach $\sim 10^{23} \text{ Wcm}^{-2}$. Therefore one can easily compensate for the $\sim 10^3$ to 10^4 suppression-factor and obtain $\sigma_{eff}^{2pa} \approx 10^{-21} \text{ cm}^2$ to 10^{-28} cm^2 with $\mathcal{P}_2 \lesssim 10^{18} \text{ Wcm}^{-2}$. A higher \mathcal{P}_2 , though achievable today, complicates the yield estimate, as target disintegration needs to be considered. Nevertheless, this process (mechanical shock-wave propagation) is much slower than the speed of light and the nuclear transition time, so pumping/depletion will still occur.

Note that the conventional treatment of $gG \approx 1/w_>$ in Eq. (6) reduces the effective cross-section due to the assumption that the beams are near *monochromatic*. This is not the case for the γ -source generated via laser-plasma interaction, as shown in Fig. 2. Unlike conventional beams, the spectrum is continuously distributed

from 1 keV to 50 MeV [119–124]. Yield estimates, in this case, require special care. The line shape of the final state does not play the same role as before, as each shifted or broaden-state will always have a combination of γ -photon plus ω -photon centered to its peak. A more convenient treatment is considering the integrated intensity of γ -photons over the energy interval equal to the total width $w_>$ of the final state. Defining such integrated intensity as ΔI_γ , as all γ -photons within that energy interval can excite the nuclei, the yield as defined in Eq. (1) becomes

$$\frac{d\mathcal{Y}_{(2)}}{dz} = N\Delta I_\gamma \frac{w_>}{\bar{w}} \sigma_{eff}^{2pa}, \quad (10)$$

with \bar{w} the bandwidth of the supplied laser.

A. Yields solely from a single γ -flash

We first investigate whether 2PA already dominates over 1PA under a single γ -flash from the laser-matter interaction. With the γ -flash alone, photons within the narrow energy range of $E_\gamma \in [1, 1.001]$ keV reach an area density of $N_\gamma \sim 10^{12}$ cm $^{-2}$ even estimated very conservatively from Fig. 2, which corresponds to $\mathcal{P}_\gamma \approx 10^9$ Wcm $^{-2}$. Plugging \mathcal{P}_γ as \mathcal{P}_2 into Eq. (8), the effective cross-section for an incoming 1 MeV γ -photon assisted by 1 keV photons becomes $\sigma_{eff}^{2pa} \approx 10^{-37}$ cm 2 . Here, σ_{eff}^{2pa} is further suppressed than previously estimated as ΔE or $E_2 \sim 1$ keV. This leads to a yield $\sim 3 \cdot 10^{-6}$ per cm in the target just by considering the combination of $E_{\gamma 1} = 1$ keV and $E_{\gamma 2} = 1$ MeV. Assuming similar N_γ persists from 1 keV to 1 MeV, then $10^6/2$ combinations are available. After summing each combination and considering the energy dependence, 10^{-4} isomers per shot are generated within 1 cm thickness in the target via 2PA. While the yields under the same condition from sequential 1PA+1PA process is 10^{-9} (assuming the cross-section at each step is 1 barn, a typical width ($\approx 10^{-4}$ eV) for the intermediate state, a negligible angular-divergence of γ , and an absence of favorable decay/feeding paths from higher-states). Thus, 2PA dominates over sequential photon absorption, considering only the γ -flash. In summary, the factors contributing to the difference in this specific case are:

- The width of the intermediate state 1PA+1PA passes through, which gives a 10^{-4} factor in its final yield with respect to the value without reduction.
- The continuous energy spectrum of the γ -flash, which enables various combinations of the photon energies within 2PA. This gives another $\approx 10^2$ enhancement in the yield from 2PA.

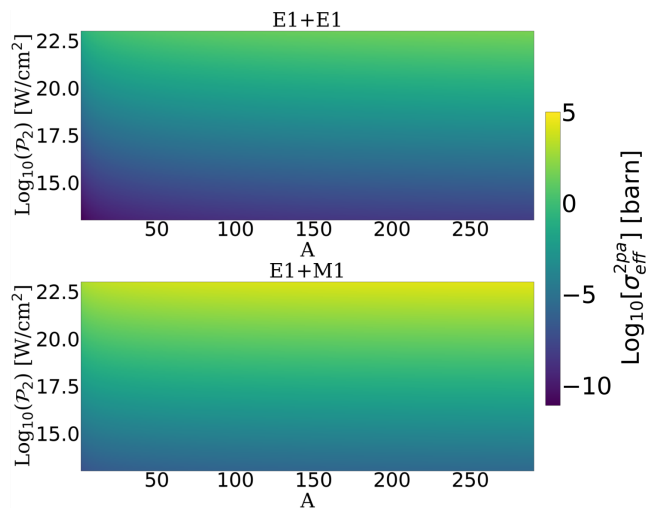


Figure 3. The 2PA effective cross section as a function of mass number A and the intensity of the supplied laser \mathcal{P}_2 , where the upper and lower panels correspond to Eq. (8) with $\Delta E = 100$ eV and Eq. (9) with $E_2 = 1$ eV, respectively. Other parameters are $E_\gamma = 1$ MeV, $\omega_> = 1$ eV, $G = 1$.

B. Yields from a combination of γ -flash and low-energy photons supplied by lasers

Combining the γ -photon with ω -photons supplied at $\mathcal{P} \gtrsim 10^{10}$ Wcm $^{-2}$ further increases the yields, as a $\gtrsim 10^3$ enhancement coming from the reduction of bandwidth from the γ -spectrum to the supplied laser, and another up to 10^6 (system-dependent) enhancement due to a smaller E_2^2 or $(\Delta E)^2$. The effective cross section currently achievable as a function of A and \mathcal{P}_2 is plotted in Fig. 3. With the setup illustrated in Fig. 1, with two modern HPLS, the number of isomers could easily reach 10^6 per shot ($\lesssim 50$ fs). In fact, we are mainly limited by the total number of γ -photons that are actually generated per absorption width, not the effective cross-section, which is sufficiently large starting from $\mathcal{P} \approx 10^{13}$ Wcm $^{-2}$ so that most of the γ 's matching the excitation energy are absorbed within 1 cm thickness in the target. Moreover, in the case of 2PA, we do not need to consider the reduction caused by the angular divergence of γ -photons as long as the whole propagation/spread stays within the target and is within the waist of the supplied laser, which is a highly desirable feature in contrast to sequential pumping.

IV. GENERALIZATION

Now, we generalize the above ingredients to enhance more transitions. First, the magnitude of the achievable σ_{eff}^{2pa} makes it possible to consider a $\langle \hat{H}_i \rangle$ of E2 type per step. A realistic E2 amplitude often exceeds the Weisskopf estimate and is suppressed only by $\sim 10^2$ relative to E1 transitions due to collective excitation [125]. Thus,

$\sigma_{eff}^{2pa,E1+E2}$ and $\sigma_{eff}^{2pa,M1+E2}$ would reach $10^{-23} \text{ cm}^2 \sim 10^{-30} \text{ cm}^2$ with \mathcal{P}_2 up to 10^{18} Wcm^{-2} , while M2 and higher multiplicities are further suppressed by at least 10^6 in their magnitude and are unfavorable. Second, it is straightforward to generalize 2PA to nPA, i.e., just re-

placing Eq. (19) by

$$R_{npa} = \frac{e^{2n} \mathcal{E}_1^2 \dots \mathcal{E}_n^2}{4^n \hbar^{2n}} |\mathcal{M}^{(n)}|^2 2\pi \delta_t(\omega - \omega_1 \dots - \omega_n), \quad (11)$$

with $\mathcal{M}^{(n)}$ as the sum over eigenstates $\langle m_2 | \sim \langle m_n |$, i.e.,

$$\mathcal{M}^{(n)} = \sum_{m_2} \dots \sum_{m_n} \left[\frac{\langle f | \hat{H}_n | m_n \rangle \dots \langle m_3 | \hat{H}_2 | m_2 \rangle \langle m_2 | \hat{H}_1 | i \rangle}{(\omega_1 - \omega_{m_2 i})(\omega_2 - \omega_{m_3 m_2}) \dots (\omega_{n-1} - \omega_{m_n m_{n-1}})} + (\text{all permutation}) \right]. \quad (12)$$

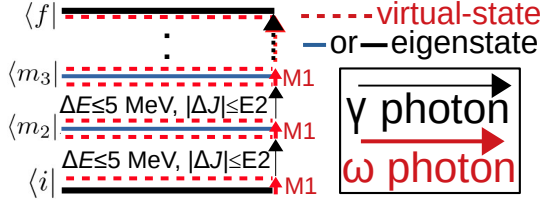


Figure 4. Illustration of an nPA scheme, where the pumping is achieved through each virtual state with gaps equal to E_{γ_i} (preferably $\lesssim 5 \text{ MeV}$) or E_{ω_i} . The “:” between $\langle m_3 |$ and $\langle f |$ corresponds to “...” in Eq. (13) and denotes similar pumping processes utilizing the $\gamma_i + \omega_i$ pairs. Only virtual states located around m_i contribute significantly.

Note that, like in Eq. (18), the adopted-intermediate state $\langle m_i |$ can be the same as $\langle i |$ or $\langle f |$. Maximum resonance occurs when each virtual state is separated from an intermediate state by the natural width of the intermediate state. A favorable scenario is that each γ_i -photon (performs E1 or E2 transition) is assisted by one ω_i -photon (performs M1 transition) to reach a virtual state, i.e.,

$$\underbrace{\gamma_1 + \omega_1}_{|\Delta J| \leq E2} + \underbrace{\gamma_2 + \omega_2}_{|\Delta J| \leq E2} + \dots, \quad (13)$$

where $|\Delta J| \leq E2$ means the transition is within $|\Delta J| \in (E1, M1, E2)$. As illustrated in Fig. 4, in general, the largest contribution facilitated by nPA would be that all of the ω -photons are used in resonating with each intermediate state via M1 transitions. Each leap with $1 \text{ keV} \lesssim \Delta E \lesssim 10 \text{ MeV}$ is completed by the γ -photons from the γ -flash, which connects intermediate states $\langle m_i |$ separated by E1, M1 or E2 transitions. The total number of intermediate states as described in Fig. 4 is $n/2 - 1$ for nPA, with the net angular momentum difference between $\langle i |$ and $\langle f |$ up to $|\Delta J| = n$. Possible modifications to the above scheme include the scenario of the existence of adjacent intermediate states separated by an energy comparable to the energy of ω -photons and with $|\Delta J^\pi| = 1^-$, which then favors an E1 transition for the ω -photons.

With the general nPA scheme in hand, we now estimate the maximum value of n that can be achieved today.

Note that the factor which governs the strength between nPA and 2PA is [126]

$$3 \cdot 10^{-24} \mathcal{P}_i \frac{X_i}{(E_\omega)^2}, \quad (14)$$

where the subscript i runs from 1 to $n - 1$ for nPA, $X_i = A^{2/3}$ (with A the total number of nucleons) if the transition carried by the i^{th} -photon is of E1 type. For M1 and E2 type transitions, X_i will be suppressed by $\gtrsim 25$ and $\gtrsim 100$ times concerning the E1 value. E_ω (in eV) represents the energy difference between each virtual state and the state it resonates with. The condition for nPA \approx (n-1)PA corresponds to Eq. (14) ≈ 1 . For $A \approx 200$, the scenario described by Fig. 4 then requires $\mathcal{P}_i \approx 10^{23} \text{ W/cm}^2$ (for both γ - and ω -photons) if $E_\omega = 1 \text{ eV}$, or $\mathcal{P}_i \approx 10^{17} \text{ W/cm}^2$ if $E_\omega = 10^{-3} \text{ eV}$. Note that $E_\omega = 10^{-3} \text{ eV}$ corresponds to a value slightly greater than the typical width of the nuclear intermediate states. To achieve such a pumping, the supplied ω -photons need to come from an intense far-infrared/terahertz source, so that the gaps between virtual states in Fig. 4 can be of the order 10^{-3} eV . A further reduction of the gaps $\lesssim 10^{-4} \text{ eV}$ would start to push the virtual states to overlap with the physical states and terminate the nPA process in the intermediate state—which can be perceived with the scenario that the two nearby red dashed-lines overlap with the blue solid-line in Fig. 4.

As shown in Fig. 2, the power density of the γ -photons—though not reaching the critical value for nPA \approx (n-1)PA—is rather intense, i.e., $\mathcal{P}_\gamma \sim 10^9 \text{ Wcm}^{-2}$ to 10^{12} Wcm^{-2} for $E_\gamma \leq 1 \text{ MeV}$. Thus, combining a typical γ -flash and ω -photons coming from another laser, 4PA can be achieved today in $A \approx 200$ nuclei with an effective cross section $\approx 10^{-25} \text{ cm}^2$. Typically, an isomer separated by $|\Delta J| \gtrsim 4$ concerning all states to which it can decay could already have a half-life $\gtrsim 1$ year, which would be accessible with our proposed population scheme in a site equipped with HPLS of PW class. Note that for isomer pumping, the J^π structure of Fig. 4 suggests that $\langle f |$ would decay easily, so $\langle f |$ is mostly a state with favorable decay paths toward the isomer state instead of the isomer itself. We note that replacing the last step in Fig. 4 by an anti-Stokes process to reach the desired isomer state is possible and can be crucial for nuclear lasers,

which we dedicated to a following work [126]. This feeding (through $\langle f|$) scheme also allows for an isomer population inversion against $\langle i|$. Counter-effects such as stimulated emissions or anti-Stokes processes are suppressed before the population of $\langle f|$ dominates.

Experimentally, only two photon sources are required: an ultra-short 10 PW laser pulse to generate γ -photons via laser-matter interactions, the other (with $\mathcal{P} \gtrsim 10^{10} \text{ Wcm}^{-2}$) supplies ω -photons. Two laser sources are sufficient because each of the ω -photons will automatically select and combine with suitable γ_i -photons presented in Fig. 2 to achieve nPA. Thus, the ω_i can be the same in Eq. (13) and be supplied by one source. Using more than one ω -source is beneficial provided that it can be tuned to another energy (away from the 1st one by at least $w_>$), then the γ -photons in another energy interval can be utilized to increase the yields.

V. EXPERIMENTAL REALIZATION

Our scheme applies to gas, liquid, and solid isomer targets. Depending on the shape/thickness of the target used to generate γ -photons, a filter which acts as a plasma mirror might be necessary to prevent the residue PW-pulses (after laser-matter interaction) from destroying a solid isomer-target. For solid isomer-targets, two scenarios can occur: (1) The target remains transparent for the ω -photons—which typically corresponds to non-metallic targets when $\mathcal{P} \lesssim 10^{11} - 10^{12} \text{ Wcm}^{-2}$. In this case, all photons penetrate the target, and no special design is required. (2) For cases where the effect of free-electrons dominates, which corresponds to metallic targets or any highly ionized target when $\mathcal{P} \gtrsim 10^{12} \text{ Wcm}^{-2}$. In this case, the ω -photons can penetrate only within a skin depth, which is usually a few nm. To maximize the yields, we need special target designs. One possibility, as sketched in Fig. 1, is a nano-wire-like structure, which allows the laser to propagate along the surface of the wires for a longer distance, and therefore maximize the yields [78, 127–146]. The realistic waist of the γ -photons is $\sim 5 \mu\text{m}$. One possibility to optimize the yield will be an array of square-type nano-wires, each with dimension $\sim 20 \text{ nm}$ on each side, and with a sufficient inter-wire distance ($\gtrsim 200 \text{ nm}$) to allow free propagation of photons.

VI. SUMMARY

Note that the fascinating idea of enhancing cross-sections by supplying various intensive beams is not new [34–37, 82, 147–155]. However, we demonstrate here for the first time that the feasibility of such a mechanism can be carried out with the help of the γ -photons generated via laser-matter interaction. Therefore, we do not need to rely on any spontaneous emission coming from the anti-Stokes or Raman process, as in those previous depletion proposals.

Moreover, previous methods utilizing sequential pumping suffer from various restrictions from the intermediate states and can be very inefficient unless there exist favorable transitions of the ground state to a higher excited state followed by its decay into the isomer state. In contrast, our scheme can be applied to pump and deplete a very wide class of nuclear isomers, and therefore represent a crucial step toward realizing exciting new concepts in nuclear photonics.

ACKNOWLEDGMENTS

We thank Paolo Tomassini and Bogdan Corobean for useful discussions and suggestions. This work was supported by the Extreme Light Infrastructure Nuclear Physics (ELI-NP) Phase II, a project co-financed by the Romanian Government and the European Union through the European Regional Development Fund - the Competitiveness Operational Programme (1/07.07.2016, COP, ID 1334); the Romanian Ministry of Research and Innovation: PN23210105 (Phase 2, the Program Nucleu), the ELI-RO grant Proiectul ELI-RO/RDI.2024.AMAP, ELI-RO.RDI.2024.LaLuThe, ELI-RO.RDI.2024.SPARC and ELI10/01.10.2020 of the Romanian Government; the European Union, the Romanian Government and the Health Program, within the project “Medical applications of high-power lasers - Dr. LASER”; SMIS Code: 326475 and the IOSIN funds for research infrastructures of national interest. We acknowledge EuroHPC Joint Undertaking for awarding us access to Karolina at IT4Innovations (VŠB-TU), Czechia, under project number OPEN-34-63 and EHPC-REG-2023R02-006 (DD-23-157), and CINECA HPC access through PRACE-ICEI standard call 2022 (P.I. Paolo Tomassini).

Conflict of Interest

The authors have no conflicts to disclose.

SUPPLEMENTAL MATERIAL

VII. DERIVATIONS OF TWO-PHOTON TRANSITION RATE

The system is perturbed by an electric field given by lasers or γ -sources consists of photons, i.e.,

$$H_{int} = \sum_{i=1}^n \mathcal{E}_i \hat{\epsilon}_i \cos[\vec{k}_i \vec{r} - \omega_i t]. \quad (15)$$

Here $|\vec{k}_i| = E_i/\hbar c$, $\omega_i = E_i/\hbar$, with E_i the energy of photons in the i^{th} -category with amplitude \mathcal{E}_i propagates in direction $\hat{\epsilon}_i$, \hbar the reduced Planck constant and c the

speed of light. t is the time. In this work we will focus on the absorption case, thus keeping only the $e^{-i\omega_i t}$ component of the cosine function in Eq. (15), and we consider each single-photon transition through intermediate states is of dipole (E1 or M1) form (i.e., expanding $e^{i\vec{k}_i \cdot \vec{r}} = 1 + i\vec{k}_i \cdot \vec{r} + \dots$ in Eq. (15) and keeping the

components up to $O(k_i \vec{r})$). Taking out the $\vec{k}_i \vec{r}$ part and denoting e as the charge, $|i\rangle$, $|m\rangle$ and $|f\rangle$ the initial, intermediate, and final state in the transition process, the transition amplitude for 2PA can then be expressed as

$$a^{[2]}(t) = \frac{e^2 \mathcal{E}_1 \mathcal{E}_2}{4\hbar^2} \sum_m \left[\frac{\langle f | \hat{H}_2 | m \rangle \langle m | \hat{H}_1 | i \rangle e^{i(\omega - \omega_1 - \omega_2)t} - 1}{\omega_1 - \omega_{mi}} + (1 \leftrightarrow 2) \right], \quad (16)$$

where the dipole interaction Hamiltonian reads

$$\begin{aligned} \hat{H}_i &= \hat{e}_i \cdot \vec{r}, & \text{for E1,} \\ &= \frac{\hbar}{2Mc} \hat{e}_i \cdot (\vec{L} + g_n \vec{S}), & \text{for M1.} \end{aligned}$$

Here M is the nucleon mass, \vec{r} , \vec{L} and \vec{S} are the spatial distance, orbital and spin angular momentum operators. g_n is the g-factor for the transition particle. The subscript in \hat{H}_i denotes that only the i^{th} component part of Eq. (15) is considered. The value $\omega = \omega_f - \omega_i$ ($\omega_{mi} = \omega_m - \omega_i$) is the energy gap between the initial and the final (intermediate) state. The term $(1 \leftrightarrow 2)$ has the same form as the first term but with 1 and 2 exchanged.

Note that here the sum over $|m\rangle$ belongs to eigenstates of the system, so that it cannot overlap with the virtual state $|\bar{v}\rangle$ with $(E_{\bar{v}} - E_i)/\hbar = \omega_1$ or ω_2 . Eq. (16) has the same form of time-dependence as 1PA, it then leads to

$$|a^{[2]}(t)|^2 = \frac{e^4 \mathcal{E}_1^2 \mathcal{E}_2^2}{16\hbar^4} |\mathcal{M}|^2 \frac{\sin^2[(\omega - \omega_1 - \omega_2)t/2]}{[(\omega - \omega_1 - \omega_2)/2]^2}, \quad (17)$$

with

$$\mathcal{M} = \sum_m \left[\frac{\langle f | \hat{H}_2 | m \rangle \langle m | \hat{H}_1 | i \rangle}{\omega_1 - \omega_{mi}} + (1 \leftrightarrow 2) \right]. \quad (18)$$

Using the same asymptotic form at $t \rightarrow \infty$ (as appeared in Fermi's golden rule) gives the following definition of transition rate

$$R_{2pa} = \frac{e^4 \mathcal{E}_1^2 \mathcal{E}_2^2}{16\hbar^4} |\mathcal{M}|^2 2\pi \delta_t(\omega - \omega_1 - \omega_2), \quad (19)$$

where δ_t has dimension of [time].

VIII. DERIVATIONS OF EFFECTIVE CROSS SECTION

With the line-shape function g given by Eq. (7) in the main text, the effective cross-section for an incoming γ -photon can be obtained by firstly replacing the δ -function in Eq. (19) by g (with \tilde{R}_{2pa} denoting this change), and

then dividing \tilde{R}_{2pa} by the flux multiplied by its velocity, i.e., $I_\gamma c$. This leads to

$$\sigma_{eff}^{2pa} = \frac{\tilde{R}_{2pa}}{I_\gamma c} G. \quad (20)$$

Using the relation $4\pi I_i \omega_i = \frac{\varepsilon_0 c}{2} |\mathbf{E}_i|^2$, where I_i is the intensity of photons and \mathbf{E}_i is the i^{th} component of Eq. (15), one has

$$\sigma_{eff}^{2pa} = (2\pi)^3 \frac{e^4 \omega_1 \omega_2}{c^2 \hbar^4 \varepsilon_0^2} I_2 |\mathcal{M}|^2 g G, \quad (21)$$

where ε_0 is the vacuum permittivity. According to Weisskopf estimates (which gives reasonable matrix elements within a factor $\sim 10^2$ with respect to experiments), the matrix element $|\langle \hat{H}_i \rangle|$ in Eq. (18) has the following form¹

$$|\langle \hat{H}_i \rangle| = \sqrt{B(\text{typ}, l_i)}, \quad (22)$$

with $B(\text{typ}, l_i)$ the reduced transition probabilities

$$B(E, l_i) = \frac{1}{4\pi} \left[\frac{3}{l_i + 3} \right]^2 R^{2l_i}, \quad (23)$$

$$B(M, l_i) = \frac{10}{\pi} \left[\frac{3}{l_i + 3} \right]^2 R^{(2l_i - 2)} \left(\frac{\hbar}{2Mc} \right)^2. \quad (24)$$

For dipole transition $l_i = 1$. Therefore $|\langle \hat{H}_i^{E1} \rangle| \approx R/4.7$, where the radius of nucleus $R \sim r_0 A^{1/3}$ with $r_0 \approx 1.2$ [fm] and A the number of nucleons. $|\langle \hat{H}_i^{M1} \rangle| \approx \frac{\sqrt{10}}{4.7} \frac{\hbar}{Mc}$.

IX. DETAILS OF THE CONVERSION IN THE γ SPECTRUM

The γ spectrum given in Fig. 2 in the main text adopts data points converted from the brilliance listed in Refs. [119-123]. Note that the brilliance, B_r , is given

¹ The index $\langle i \rangle$, $\langle f \rangle$ and $\langle m \rangle$ are dropped as the detailed wavefunction no longer matters in Weisskopf estimates.

in unit $[\text{s}^{-1}\text{mm}^{-2}\text{mrad}^{-2}(0.1\% \text{BW})^{-1}]$. Meanwhile, the crucial quantity is the flux of the photons per bandwidth (BW) coming out from the initial area they were generated. Nevertheless, the conversion is straightforward, provided that the duration of the γ -photons and the actual angular spread of the beam (denoted as θ here) are given. Denoting N_γ (in the unit $[\text{eV}^{-1}\text{cm}^{-2}]$) the areal density of photons accumulated within 1 eV interval at a given energy E_γ , one has

$$N_\gamma = \frac{B_r \times [\text{duration in fs}] \times [\theta \text{ in mrad}]^2}{10^{15} \times [10^{-3} E_\gamma \text{ in eV}]} 10^2. \quad (25)$$

Note that the curve in Fig. 2 is produced by an exponential fit from the data of Ref. [119] at $E_\gamma = 1, 10$ and 100 MeV. However, only at $E_\gamma = 1$ MeV, $\theta = 0.7$ [rad] is given. We have therefore assumed that the same θ applies for other energies². Thus, the black curve shown in Fig. 2 could be subjected to an uncertainty up to 10 times for $E_\gamma \gtrsim 10$ MeV in the worst scenario. Similarly, for Refs. [120-123], the value of θ is adopted whenever directly available or by interpreting its value from relevant plots (i.e., those showing the angular divergence of the beam).

X. PRACTICAL SCENARIOS OF THE HPLS-BASED γ - AND ISOMER-PRODUCTION

To enable our isomer pumping/depletion scheme, one of the prerequisites is a high-density γ -flash, which can be given by the interaction between high-power laser pulses and matter. Although laser wakefield acceleration [156, 157] based radiation schemes [158] such as bremsstrahlung and betatron radiation are specific alternatives, shooting a high-power laser pulse onto an overdense target may be the preferred approach because of the higher yields of γ -photons per eV interval, which can reach an areal density $N_\gamma \sim 10^{12} \text{eV}^{-1}\text{cm}^{-2}$ for $E_\gamma \approx 1 \text{keV} \sim 5 \text{MeV}$, as extracted very conservatively (Ref.[119] suggests $N_\gamma \sim 10^{14} \text{eV}^{-1}\text{cm}^{-2}$ for the same interval) from Fig. 2 in the main text.

This mechanism starts with a laser pulse of a wavelength of $\lambda \sim 1 \mu\text{m}$ that is compressed through the chirped pulse amplification technique [159] into a time scale of $\sim 25 \text{fs}$ to 50fs to achieve intensities up to $\mathcal{P} \sim 10^{21} \text{Wcm}^{-2}$ to $\mathcal{P} \sim 10^{23} \text{Wcm}^{-2}$. Such an ultraintense infrared pulse then interacts with a solid target and ionizes its electrons, forming a plasma environment. Consequently, this laser-matter interaction accelerates part of the electrons to relativistic energies.

These pre-accelerated electrons then interact with the laser field, emitting the high energy radiation, typically via the non-linear Thomson or Compton scattering mechanisms. Multiple schemes for generating dense

γ -photons exist and are cited as [119-123] in the main text. In those schemes, the temporal contrast of the HPLS can significantly influence the properties of generated γ -flash. However, there are techniques to improve the contrast, as for instance the plasma mirror, although at the expense of the main pulse energy. Ref. [119] in the main text suggests a 10-fold reduction of the γ -flux if the laser power is reduced from 10 PW to 3 PW. In this scenario, the data represented in Fig. 2 of the main text can practically be rescaled accordingly.

During the generation of γ -photons, particles such as electrons, low-energy (i.e., eV-level) photons, ions, and target debris are usually produced. Although charged particles could potentially contribute to isomer pumping/depletion (e.g., via Coulomb excitation) and might be desirable, they could also destroy a solid-type isomer target. The most straightforward way to sufficiently attenuate the population of eV-level photons and charged particles, block the debris, and prevent crucial damage to the isomer target is to place a solid filter between the target of laser-matter interaction and the isomer target. As illustrated in Fig. 1 in the main text, such a filter also serves as a plasma mirror to absorb/reflect/scatter the laser light.

A filter of about 1 mm thickness or more (e.g., 1 mm Tungsten) is sufficient to stop the high population of low-energy particles, which can cause damage to the isomer target. Such a filter would still have a negligible effect in absorbing the γ -flash. However, the inclusion of such a filter will increase the distance between the γ -photon source and isomer target; hence, it is sensible to minimize its thickness using, for instance, high- Z materials.

Note that a crucial advantage of our scheme is that the ω -photons coming from the supplied laser are not required to be aligned to the γ -photons for multi-photon absorption to occur, although the spatial overlap between γ -photons, ω -photons, and the isomer target is of the essence. The beam quality of the γ -photons determines the achievable overlap. PIC simulations (Refs. [119-123]) suggest that the majority of the γ -photons are generated from an initial area $\sim 10 \mu\text{m} \times 10 \mu\text{m}$ and exhibit an angular divergence $\theta \sim 30$ deg. Therefore, the flux would be reduced by a factor ~ 2000 after propagating ~ 1 mm. In any case, assuming a $\sim 2000\times$ diluted γ -intensity is still remediable by the supplied ω -photons³, the supplied laser needs to be adjusted to have a waist $w_0 \gtrsim 250 \mu\text{m}$ to cover the entire path of the γ -photons up to a distance ≈ 1 mm. This is very achievable even with TW-class laser systems and a long focal mirror to achieve a focused beam with a large focal spot and several mm of Rayleigh length. Owing to the waist size and Rayleigh length larger than the region of laser-matter interaction, the TW laser can be placed either on the side facing the

² Normally, θ would be lower for higher energies.

³ The divergence of γ -photons plays no role for a 2PA of $\omega + \gamma$ type, but it matters when more than one γ enters the nPA.

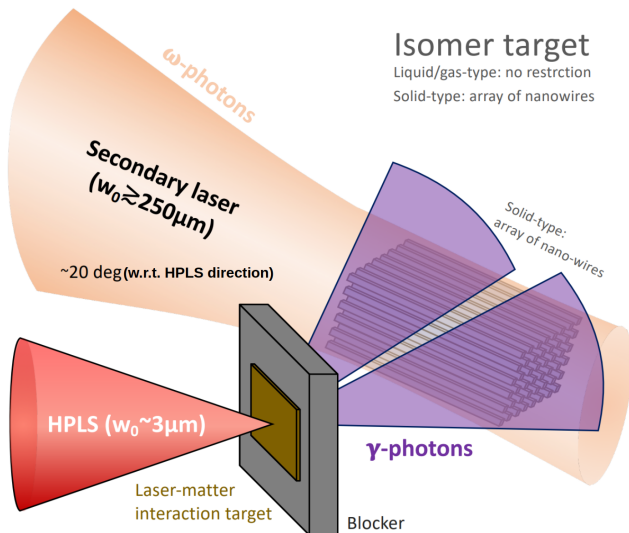


Figure 5. Illustration of an experimental setup. A γ -flash driven by the main HPLS pulse typically has two main lobes, where the isomer targets are placed correspondingly. If the isomer target is of solid form, a nano-wire-like structure is preferred (with their detailed structure illustrated in Fig. 1 of the main text), and the ω -photons need to be aligned to the nano-wires, which may be placed to have an angle ~ 20 deg with respect to the HPLS direction. If the isomer target is of gas or liquid form, all restrictions can be levitated in favoring a maximum overlap volume between the γ - and ω -photons.

laser-matter interaction (slightly non-parallel to the direction of HPLS, as illustrated in Fig. 5 above), or on the opposite side—where it is allowed to propagate anti-parallelly with respect to the HPLS⁴.

One remaining factor in the practical realization concerns the practical target design to maximize the isomer yields. As mentioned in the main text, if eV-level ω -photons are adopted, with $\mathcal{P} \gtrsim 10^{12} \text{ Wcm}^{-2}$, they can only penetrate solid targets up to a skin depth ~ 5 nm. In this case, an array with a nano-wire-like structure for the isomer target is preferred. As illustrated in Fig. 1 in the main text, we estimate the dimension of each side of the nano-wire to be ~ 20 nm, and an inter-wire spacing of $\gtrsim 200$ nm. This will allow ω -photons to propagate through the entire isomer target without being blocked or reflected by the nano-wires.

Finally, it is worth noting that the above setup and restrictions regarding the isomer pumping have relevance *only* to a solid target and *only* in the case where one wishes to keep its original shape in favor of pumping/depletion with continuous cycles. In general, gas or liquid forms of isomers or a one-time-use solid target can be employed with a much simpler experimental setup.

-
- [1] Mark A. Prelas, Charles L. Weaver, Matthew L. Watermann, Eric D. Lukosi, Robert J. Schott, et al., “A review of nuclear batteries,” *Progress in Nuclear Energy* **75**, 117–148 (2014).
 - [2] Cornelia Nitipir, Dana Niculae, Cristina Orlov, Maria Barbu, Bogdan Popescu, et al., “Update on radionuclide therapy in oncology (review),” *Oncology Letters* (2017), 10.3892/ol.2017.7141.
 - [3] Nienke J. M. Klaassen, Mark J. Arntz, Alexandra Gil Arranja, Joey Roosen, and J. Frank W. Nijsen, “The various therapeutic applications of the medical isotope holmium-166: a narrative review,” *EJNMMI Radiopharmacy and Chemistry* **4** (2019), 10.1186/s41181-019-0066-3.
 - [4] George Sgouros, Lisa Bodei, Michael R. McDevitt, and Jessie R. Nedrow, “Radiopharmaceutical therapy in cancer: clinical advances and challenges,” *Nature Reviews Drug Discovery* **19**, 589–608 (2020).
 - [5] George C. Baldwin, Johndale C. Solem, and Vitalii I. Gol’danskii, “Approaches to the development of gamma-ray lasers,” *Rev. Mod. Phys.* **53**, 687–744 (1981).
 - [6] George C. Baldwin and Johndale C. Solem, “Recoilless gamma-ray lasers,” *Rev. Mod. Phys.* **69**, 1085–1118 (1997).
 - [7] Otto Hahn, “ber ein neues radioaktives zerfallsprodukt im uran,” *Die Naturwissenschaften* **9**, 84–84 (1921).
 - [8] Philip Walker and George Dracoulis, “Energy traps in atomic nuclei,” *Nature* **399**, 35–40 (1999).
 - [9] J. Tiedau, M. V. Okhapkin, K. Zhang, J. Thielking, G. Zitzer, et al., “Laser excitation of the th-229 nucleus,” *Phys. Rev. Lett.* **132**, 182501 (2024).
 - [10] S. A. Karamian and J. J. Carroll, “Cross section for inelastic neutron “acceleration” by $^{178}\text{Hf}^{m2}$,” *Phys. Rev. C* **83**, 024604 (2011).
 - [11] Jie Feng, Wenzhao Wang, Changbo Fu, Liming Chen, Junhao Tan, et al., “Femtosecond pumping of nuclear isomeric states by the coulomb collision of ions with quivering electrons,” *Physical Review Letters* **128** (2022), 10.1103/physrevlett.128.052501.
 - [12] C. J. Chiara, J. J. Carroll, M. P. Carpenter, J. P. Greene, D. J. Hartley, et al., “Isomer depletion as experimental evidence of nuclear excitation by electron capture,” *Nature* **554**, 216–218 (2018).
 - [13] Song Guo, Yongde Fang, Xiaohong Zhou, and C. M. Petrache, “Possible overestimation of isomer depletion due to contamination,” *Nature* **594**, E1–E2 (2021).
 - [14] S. Guo, B. Ding, X. H. Zhou, Y. B. Wu, J. G. Wang, et al., “Probing ^{93m}Mo isomer depletion with an isomer beam,” *Phys. Rev. Lett.* **128**, 242502 (2022).
 - [15] Yuanbin Wu, Christoph H. Keitel, and Adriana Pálffy, “ ^{93m}Mo isomer depletion via beam-based nuclear excitation by electron capture,” *Phys. Rev. Lett.* **122**, 212501 (2019).

⁴ In this case, the base where nano-wires are planted will be shifted to the HPLS side and integrate with the plasma mirror.

- [16] V.I. Goldanskii and V.A. Namiot, “On the excitation of isomeric nuclear levels by laser radiation through inverse internal electron conversion,” *Physics Letters B* **62**, 393–394 (1976).
- [17] P. Morel, “Nuclear excitation by electronic processes: NEEC and NEEF effects,” *AIP Conference Proceedings* (2005), 10.1063/1.1945195.
- [18] Adriana Pálffy, Jörg Evers, and Christoph H. Keitel, “Isomer triggering via nuclear excitation by electron capture,” *Phys. Rev. Lett.* **99**, 172502 (2007).
- [19] D. Belic, C. Arlandini, J. Besserer, J. de Boer, J. J. Carroll, et al., “Photoactivation of $^{180}\text{Ta}^m$ and its implications for the nucleosynthesis of nature’s rarest naturally occurring isotope,” *Phys. Rev. Lett.* **83**, 5242–5245 (1999).
- [20] I. Stefanescu, G. Georgiev, F. Ames, J. Äystö, D. L. Balabanski, et al., “Coulomb excitation of $^{68,70}\text{Cu}$: First use of postaccelerated isomeric beams,” *Phys. Rev. Lett.* **98**, 122701 (2007).
- [21] O. Roig, V. Méot, B. Rossé, G. Bélier, J.-M. Daugas, et al., “Direct evidence for inelastic neutron “acceleration” by $^{177}\text{Lu}^m$,” *Phys. Rev. C* **83**, 064617 (2011).
- [22] J. J. Carroll, M. S. Litz, K. A. Netherton, S. L. Henriquez, N. R. Pereira, et al., “Nuclear structure and depletion of nuclear isomers using electron linacs,” *AIP Conference Proceedings* (2013), 10.1063/1.4802396.
- [23] V.I. Kirischuk, V.A. Ageev, A.M. Dovbnya, S.S. Kandybei, and Yu.M. Ranyuk, “Induced acceleration of the decay of the 31-yr isomer of 178m2 hf using bremsstrahlung radiation,” *Physics Letters B* **750**, 89–94 (2015).
- [24] Lars von der Wense, Benedict Seiferle, Mustapha Laatiaoui, Jürgen B. Neumayr, Hans-Jörg Maier, et al., “Direct detection of the 229th nuclear clock transition,” *Nature* **533**, 47–51 (2016).
- [25] J.J. Carroll, S.A. Karamian, R. Propri, D. Gohlke, N. Caldwell, et al., “Search for low-energy induced depletion of 178hf2 at the SPring-8 synchrotron,” *Physics Letters B* **679**, 203–208 (2009).
- [26] Jonas Gunst, Yuanbin Wu, Christoph H. Keitel, and Adriana Pálffy, “Nuclear excitation by electron capture in optical-laser-generated plasmas,” *Phys. Rev. E* **97**, 063205 (2018).
- [27] Yuanbin Wu, Jonas Gunst, Christoph H. Keitel, and Adriana Pálffy, “Tailoring laser-generated plasmas for efficient nuclear excitation by electron capture,” *Phys. Rev. Lett.* **120**, 052504 (2018).
- [28] J. Rzadkiewicz, M. Polasik, K. Ślabkowska, L. Syrocki, J. J. Carroll, et al., “Novel approach to ^{93m}Mo isomer depletion: Nuclear excitation by electron capture in resonant transfer process,” *Phys. Rev. Lett.* **127**, 042501 (2021).
- [29] Silviu Olariu and Agata Olariu, “Induced emission of γ radiation from isomeric nuclei,” *Phys. Rev. C* **58**, 333–336 (1998).
- [30] Silviu Olariu and Agata Olariu, “Power densities for two-step γ -ray transitions from isomeric states,” *Phys. Rev. C* **58**, 2560–2562 (1998).
- [31] P. M. Walker, G. D. Dracoulis, and J. J. Carroll, “Interpretation of the excitation and decay of $^{180}\text{Ta}^m$ through a $K^\pi = 5^+$ band,” *Phys. Rev. C* **64**, 061302(R) (2001).
- [32] Eugene V. Tkalya, “Induced decay of $^{178}\text{Hf}^{m2}$: Theoretical analysis of experimental results,” *Phys. Rev. C* **71**, 024606 (2005).
- [33] K. M. Spohr et al., “On the possibility of laser-plasma-induced depopulation of the isomer in ^{93}Mo at ELI-NP,” *Eur. Phys. J. A* **59**, 281 (2023).
- [34] S. Olariu, Iovitzu Popescu, and C. B. Collins, “Tuning of γ -ray processes with high power optical radiation,” *Phys. Rev. C* **23**, 50–63 (1981).
- [35] C. B. Collins, S. Olariu, M. Petrascu, and Iovitzu Popescu, “Laser-induced resonant absorption of γ radiation,” *Phys. Rev. C* **20**, 1942–1945 (1979).
- [36] S. Olariu, Iovitzu Popescu, and C. B. Collins, “Multi-photon generation of optical sidebands to nuclear transitions,” *Phys. Rev. C* **23**, 1007–1014 (1981).
- [37] W. Becker, R. R. Schlicher, and M. O. Scully, “Comment on enhancement of forbidden nuclear beta decay by high-intensity radio-frequency fields,” *Phys. Rev. C* **29**, 1124–1131 (1984).
- [38] Wu Wang, Jie Zhou, Boqun Liu, and Xu Wang, “Exciting the isomeric ^{229}Th nuclear state via laser-driven electron recollision,” *Phys. Rev. Lett.* **127**, 052501 (2021).
- [39] Wenjuan Lv, Hao Duan, and Jie Liu, “Enhanced deuterium-tritium fusion cross sections in the presence of strong electromagnetic fields,” *Phys. Rev. C* **100**, 064610 (2019).
- [40] S. A. Ghinescu and D. S. Delion, “Coupled-channels analysis of the α decay in strong electromagnetic fields,” *Phys. Rev. C* **101**, 044304 (2020).
- [41] Lars von der Wense, Pavlo V Bilous, Benedict Seiferle, Simon Stellmer, Johannes Weitenberg, et al., “The theory of direct laser excitation of nuclear transitions,” *The European Physical Journal A* **56**, 176 (2020).
- [42] Xu Wang, “Nuclear excitation of ^{229}Th induced by laser-driven electron recollision,” *Phys. Rev. C* **106**, 024606 (2022).
- [43] John Jasper Bekx, Martin Louis Lindsey, Siegfried Heinz Glenzer, and Karl-Georg Schlesinger, “Applicability of semiclassical methods for modeling laser-enhanced fusion rates in a realistic setting,” *Phys. Rev. C* **105**, 054001 (2022).
- [44] Jintao Qi, Tao Li, Ruihua Xu, Libin Fu, and Xu Wang, “ α decay in intense laser fields: Calculations using realistic nuclear potentials,” *Phys. Rev. C* **99**, 044610 (2019).
- [45] Friedemann Queisser and Ralf Schützhold, “Dynamically assisted nuclear fusion,” *Phys. Rev. C* **100**, 041601(R) (2019).
- [46] Tao Li and Xu Wang, “Nonlinear optical effects in a nucleus,” *Journal of Physics G: Nuclear and Particle Physics* **48**, 095105 (2021).
- [47] Shiwei Liu, Hao Duan, Difa Ye, and Jie Liu, “Deuterium-tritium fusion process in strong laser fields: Semiclassical simulation,” *Phys. Rev. C* **104**, 044614 (2021).
- [48] Wenjuan Lv, Binbing Wu, Hao Duan, Shiwei Liu, and Jie Liu, “Phase-dependent cross sections of deuterium-tritium fusion in dichromatic intense fields with high-frequency limit,” *The European Physical Journal A* **58** (2022), 10.1140/epja/s10050-022-00697-8.
- [49] Haowei Xu, Hao Tang, Guoqing Wang, Changhao Li, Boning Li, et al., “Solid-state ^{229}Th nuclear laser with two-photon pumping,” *Phys. Rev. A* **108**, L021502 (2023).
- [50] Zhi-Wei Lu, Liang Guo, Zheng-Zheng Li, Mamutjan

- Ababekri, Fang-Qi Chen, Changbo Fu, Chong Lv, Ruirui Xu, Xiangjin Kong, Yi-Fei Niu, and Jian-Xing Li, “Manipulation of giant multipole resonances via vortex γ photons,” *Phys. Rev. Lett.* **131**, 202502 (2023).
- [51] Jin Woo Yoon, Cheonha Jeon, Junghoon Shin, Seong Ku Lee, Hwang Woon Lee, et al., “Achieving the laser intensity of $5.5 \times 10^{22} \text{ W/cm}^2$ with a wavefront-corrected multi-PW laser,” *Opt. Express* **27**, 20412–20420 (2019).
- [52] Jin Woo Yoon, Yeong Gyu Kim, Il Woo Choi, Jae Hee Sung, Hwang Woon Lee, et al., “Realization of laser intensity over 10^{23} W/cm^2 ,” *Optica* **8**, 630–635 (2021).
- [53] Wenqi Li, Zebiao Gan, Lianghong Yu, Cheng Wang, Yanqi Liu, et al., “339 J high-energy ti:sapphire chirped-pulse amplifier for 10PW laser facility,” *Opt. Lett.* **43**, 5681–5684 (2018).
- [54] Linpeng Yu, Yi Xu, Yanqi Liu, Yanyan Li, Shuai Li, et al., “High-contrast front end based on cascaded xpwg and femtosecond opa for 10-pw-level ti:sapphire laser,” *Opt. Express* **26**, 2625–2633 (2018).
- [55] CA Ur, D Balabanski, G Cata-Danil, S Gales, I Morjan, et al., “The eli-np facility for nuclear physics,” *Nuclear Instruments and Methods in Physics Research Section B: Beam Interactions with Materials and Atoms* **355**, 198–202 (2015).
- [56] K. A. Tanaka, K. M. Spohr, D. L. Balabanski, S. Balascuta, L. Capponi, et al., “Current status and highlights of the ELI-NP research program,” *Matter and Radiation at Extremes* **5** (2020), 10.1063/1.5093535.
- [57] Tatsufumi Nakamura, James K. Koga, Timur Zh. Esirkepov, Masaki Kando, Georg Korn, et al., “High-power γ -ray flash generation in ultraintense laser-plasma interactions,” *Phys. Rev. Lett.* **108**, 195001 (2012).
- [58] C. P. Ridgers, C. S. Brady, R. Ducloux, J. G. Kirk, K. Bennett, et al., “Dense electron-positron plasmas and ultraintense γ rays from laser-irradiated solids,” *Phys. Rev. Lett.* **108**, 165006 (2012).
- [59] L. L. Ji, A. Pukhov, E. N. Nerush, I. Yu. Kostyukov, B. F. Shen, et al., “Energy partition, gamma-ray emission, and radiation reaction in the near-quantum electrodynamic regime of laser-plasma interaction,” *Physics of Plasmas* **21**, 023109 (2014).
- [60] T. G. Blackburn, C. P. Ridgers, J. G. Kirk, and A. R. Bell, “Quantum radiation reaction in laser–electron-beam collisions,” *Phys. Rev. Lett.* **112**, 015001 (2014).
- [61] Jian-Xing Li, Karen Z. Hatsagortsyan, Benjamin J. Gallow, and Christoph H. Keitel, “Attosecond gamma-ray pulses via nonlinear compton scattering in the radiation-dominated regime,” *Phys. Rev. Lett.* **115**, 204801 (2015).
- [62] H. X. Chang, B. Qiao, T. W. Huang, Z. Xu, C. T. Zhou, et al., “Brilliant petawatt gamma-ray pulse generation in quantum electrodynamic laser-plasma interaction,” *Scientific Reports* **7** (2017), 10.1038/srep45031.
- [63] Xing-Long Zhu, Min Chen, Tong-Pu Yu, Su-Ming Weng, Li-Xiang Hu, et al., “Bright attosecond gamma-ray pulses from nonlinear compton scattering with laser-illuminated compound targets,” *Applied Physics Letters* **112** (2018), 10.1063/1.5028555.
- [64] T W Huang, C M Kim, C T Zhou, M H Cho, K Nakajima, et al., “Highly efficient laser-driven compton gamma-ray source,” *New Journal of Physics* **21**, 013008 (2019).
- [65] F. Mackenroth and A. Di Piazza, “Nonlinear compton scattering in ultrashort laser pulses,” *Phys. Rev. A* **83**, 032106 (2011).
- [66] A. Gonoskov, A. Bashinov, S. Bastrakov, E. Efimenko, A. Ilderton, et al., “Ultrabright gev photon source via controlled electromagnetic cascades in laser-dipole waves,” *Phys. Rev. X* **7**, 041003 (2017).
- [67] J. Snyder, L. L. Ji, K. M. George, C. Willis, G. E. Cochran, et al., “Relativistic laser driven electron accelerator using micro-channel plasma targets,” *Physics of Plasmas* **26** (2019), 10.1063/1.5087409.
- [68] Xiaofei Shen, Alexander Pukhov, and Bin Qiao, “High-flux bright x-ray source from femtosecond laser-irradiated microtapes,” *Communications Physics* **7** (2024), 10.1038/s42005-024-01575-z.
- [69] N. Tsoneva, Ch. Stoyanov, Yu. P. Gangrsky, V. Yu. Ponomarev, N. P. Balabanov, et al., “Population of isomers in the decay of the giant dipole resonance,” *Phys. Rev. C* **61**, 044303 (2000).
- [70] Jie Feng, Yaojun Li, Junhao Tan, Wenzhao Wang, Yifei Li, et al., “Laser plasma-accelerated ultra-intense electron beam for efficiently exciting nuclear isomers,” *Laser & Photonics Reviews* (2023), 10.1002/lpor.202300514.
- [71] M. Borghesi, J. Fuchs, S. V. Bulanov, A. J. MacKinnon, P. K. Patel, et al., “Fast ion generation by high-intensity laser irradiation of solid targets and applications,” *Fusion Science and Technology* **49**, 412–439 (2006).
- [72] M. Roth, A. Blazevic, M. Geissel, T. Schlegel, T. E. Cowan, et al., “Energetic ions generated by laser pulses: A detailed study on target properties,” *Phys. Rev. ST Accel. Beams* **5**, 061301 (2002).
- [73] B Grant Logan, Roger O Bangerter, Debra A Callahan, Max Tabak, Markus Roth, et al., “Assessment of potential for ion-driven fast ignition,” *Fusion science and technology* **49**, 399–411 (2006).
- [74] M Roth, “Review on the current status and prospects of fast ignition in fusion targets driven by intense, laser generated proton beams,” *Plasma Physics and Controlled Fusion* **51**, 014004 (2008).
- [75] X. F. Shen, A. Pukhov, and B. Qiao, “Monoenergetic high-energy ion source via femtosecond laser interacting with a microtape,” *Phys. Rev. X* **11**, 041002 (2021).
- [76] J Sarma, A McIlvenny, N Das, M Borghesi, and A Macchi, “Surface plasmon-driven electron and proton acceleration without grating coupling,” *New Journal of Physics* **24**, 073023 (2022).
- [77] Q. S. Wang, C. Y. Qin, H. Zhang, S. Li, A. X. Li, et al., “Spatial distribution modulation of laser-accelerated charged particles with micro-tube structures,” *Physics of Plasmas* **30** (2023), 10.1063/5.0138179.
- [78] E. Eftekhari-Zadeh, M. S. Blümcke, Z. Samsonova, R. Loetzsch, I. Uschmann, et al., “Laser energy absorption and x-ray generation in nanowire arrays irradiated by relativistically intense ultra-high contrast femtosecond laser pulses,” *Physics of Plasmas* **29** (2022), 10.1063/5.0064364.
- [79] Yuan Zhao, Haiyang Lu, Cangtao Zhou, and Jungao Zhu, “Overcritical electron acceleration and betatron radiation in the bubble-like structure formed by re-injected electrons in a tailored transverse plasma,” *Matter and Radiation at Extremes* **8** (2022), 10.1063/5.0121558.
- [80] Maria Göppert-Mayer, “Über elementarakte mit zwei

- quantensprünge,” *Annalen der Physik* **401**, 273–294 (1931).
- [81] W. Kaiser and C. G. B. Garrett, “Two-photon excitation in $\text{CaF}_2: \text{Eu}^{2+}$,” *Phys. Rev. Lett.* **7**, 229–231 (1961).
- [82] C. B. Collins, S. Olariu, M. Petrascu, and Iovitzu Popescu, “Enhancement of γ -ray absorption in the radiation field of a high-power laser,” *Phys. Rev. Lett.* **42**, 1397–1400 (1979).
- [83] C. B. Collins, F. W. Lee, D. M. Shemwell, B. D. DePaola, S. Olariu, et al., “The coherent and incoherent pumping of a gamma ray laser with intense optical radiation,” *Journal of Applied Physics* **53**, 4645–4651 (1982).
- [84] C.-J. Yang, V. Horny, D. Doria, and K. Spohr, “Nuclear physics under the low-energy, high-intensity frontier,” Proc. SPIE 13535, Research Using Extreme Light Infrastructures: New Frontiers with Petawatt-Level Lasers VI, 1353506 (2025).
- [85] J. Schirmer, D. Habs, R. Kroth, N. Kwong, D. Schwalm, et al., “Double gamma decay in ^{40}Ca and ^{90}Zr ,” *Phys. Rev. Lett.* **53**, 1897–1900 (1984).
- [86] J. Kramp, D. Habs, R. Kroth, M. Music, J. Schirmer, et al., “Nuclear two-photon decay in $0^+ \rightarrow 0^+$ transitions,” *Nuclear Physics A* **474**, 412–450 (1987).
- [87] S. Gorodetzky, G. Sutter, R. Armbruster, P. Chevallier, P. Mennrath, et al., “Double gamma emission in the 6.06-MeV monopole transition of O^{16} ,” *Phys. Rev. Lett.* **7**, 170–172 (1961).
- [88] D. E. Alburger and P. D. Parker, “Search for double gamma-ray emission from the first excited states of O^{16} and C^{12} ,” *Physical Review* **135**, B294–B300 (1964).
- [89] P. Harihar, J. D. Ullman, and C. S. Wu, “Search for double gamma emission from the first excited states of Ca^{40} and Zr^{90} ,” *Physical Review C* **2**, 462–467 (1970).
- [90] Yasuyuki Nakayama, “Two-photon decay of the 1.76-MeV 0^+ state of ^{90}Zr ,” *Physical Review C* **7**, 322–330 (1973).
- [91] J. C. Vanderleeden and P. S. Jastram, “Search for Double-Photon Decay in Zr^{90} ,” *Phys. Rev. C* **1**, 1025–1035 (1970).
- [92] P. A. Söderström, L. Capponi, E. Açıksöz, T. Otsuka, N. Tsoneva, et al., “Electromagnetic character of the competitive $\gamma\gamma/\gamma$ -decay from ^{137m}Ba ,” *Nature Commun.* **11**, 3242 (2020), arXiv:2001.00554 [nucl-ex].
- [93] D. Freire-Fernández, W. Korten, R. J. Chen, S. Litvinov, Yu. A. Litvinov, et al., “Measurement of the isolated nuclear two-photon decay in ^{72}Ge ,” (2023), arXiv:2312.11313 [nucl-ex].
- [94] P. Lambropoulos, “Topics on multiphoton processes in atoms**work supported by a grant from the national science foundation no. mps74-17553.” (Academic Press, 1976) pp. 87–164.
- [95] Harald Friedrich, *Theoretical Atomic Physics* (Springer International Publishing, 2017).
- [96] Nikolai B. Delone and Vladimir P. Krainov, *Multiphoton Processes in Atoms* (Springer Berlin Heidelberg, 2000).
- [97] “<https://doi.org/10.60893/figshare.mre.c.7907990.v1>,” .
- [98] WR Johnson, CD Lin, KT Cheng, and CM Lee, “Relativistic random-phase approximation,” *Physica Scripta* **21**, 409 (1980).
- [99] John C Slater, “A simplification of the hartree-fock method,” *Physical Review* **81**, 385 (1951).
- [100] Charlotte Froese-Fischer, T. Brage, and P. Jonsson, *Computational Atomic Structure: An MCHF Approach* (Routledge, 2019).
- [101] Stephen Wilson, “Diagrammatic many-body perturbation theory of atomic and molecular electronic structure,” *Computer Physics Reports* **2**, 391–480 (1985).
- [102] Steven T Manson, “Relativistic-random-phase approximation calculations of atomic photoionization: what we have learned,” *Canadian Journal of Physics* **87**, 5–8 (2009).
- [103] K. Omidvar, “Two-photon excitation cross section in light and intermediate atoms in frozen-core LS-coupling approximation,” *Phys. Rev. A* **22**, 1576–1587 (1980).
- [104] K. Omidvar, “Erratum: Two-photon excitation cross section in light and intermediate atoms in frozen-core LS-coupling approximation,” *Phys. Rev. A* **30**, 2805(E) (1984).
- [105] Roberta P. Saxon and Jörg Eichler, “Theoretical calculation of two-photon absorption cross sections in atomic oxygen,” *Phys. Rev. A* **34**, 199–206 (1986).
- [106] Douglas J. Bamford, Leonard E. Jusinski, and William K. Bischel, “Absolute two-photon absorption and three-photon ionization cross sections for atomic oxygen,” *Phys. Rev. A* **34**, 185–198 (1986).
- [107] G Mainfray and G Manus, “Multiphoton ionization of atoms,” *Reports on Progress in Physics* **54**, 1333–1372 (1991).
- [108] CB Collins and JJ Carroll, “Progress in the pumping of gamma-ray laser,” *Hyperfine interactions* **107**, 3–42 (1997).
- [109] L. Krauss-Kodytek, W.-R. Hannes, T. Meier, C. Rupert, and M. Betz, “Nondegenerate two-photon absorption in zns: Experiment and theory,” *Phys. Rev. B* **104**, 085201 (2021).
- [110] U. van Kolck, “The Problem of Renormalization of Chiral Nuclear Forces,” *Front. in Phys.* **8**, 79 (2020).
- [111] C. J. Yang, “Do we know how to count powers in pionless and pionful effective field theory?” *Eur. Phys. J. A* **56**, 96 (2020).
- [112] C. J. Yang, A. Ekström, C. Forssén, G. Hagen, G. Ruppak, L. Capponi, E. Açıksöz, T. Otsuka, and N. and Tsoneva, “The importance of few-nucleon forces in chiral effective field theory,” *Eur. Phys. J. A* **59**, 233 (2023).
- [113] Ingo Tews et al., “Nuclear Forces for Precision Nuclear Physics: A Collection of Perspectives,” *Few Body Syst.* **63**, 67 (2022).
- [114] John Markus Blatt and Victor Frederick Weisskopf, *Theoretical nuclear physics* (Springer, New York, 1952).
- [115] G. S. Agarwal, “Field-correlation effects in multiphoton absorption processes,” *Phys. Rev. A* **1**, 1445–1459 (1970).
- [116] P Zoller and P Lambropoulos, “Laser temporal coherence effects in two-photon resonant three-photon ionisation,” *Journal of Physics B: Atomic and Molecular Physics* **13**, 69–83 (1980).
- [117] M. N. Hack and M. Hamermesh, “Effect of radiofrequency resonance on the natural line form,” *Il Nuovo Cimento* **19**, 546–557 (1961).
- [118] Rudolf L. Mössbauer, “Kernresonanzfluoreszenz von gammastrahlung in ir^{191} ,” *Zeitschrift für Physik* **151**, 124–143 (1958).
- [119] T. Wang, X. Ribeyre, Z. Gong, O. Jansen, E. d’Humières, et al., “Power scaling for collimated γ -

- ray beams generated by structured laser-irradiated targets and its application to two-photon pair production,” *Phys. Rev. Appl.* **13**, 054024 (2020).
- [120] Yan-Jun Gu, Ondrej Klimo, Sergei V. Bulanov, and Stefan Weber, “Brilliant gamma-ray beam and electron–positron pair production by enhanced attosecond pulses,” *Communications Physics* **1** (2018), 10.1038/s42005-018-0095-3.
- [121] Kun Xue, Zhen-Ke Dou, Feng Wan, Tong-Pu Yu, Wei-Min Wang, et al., “Generation of highly-polarized high-energy brilliant gamma-rays via laser-plasma interaction,” *Matter and Radiation at Extremes* **5** (2020), 10.1063/5.0007734.
- [122] Tao Wang, David Blackman, Katherine Chin, and Alexey Arefiev, “Effects of simulation dimensionality on laser-driven electron acceleration and photon emission in hollow microchannel targets,” *Phys. Rev. E* **104**, 045206 (2021).
- [123] Christian Heppel and Naveen Kumar, “High brilliance γ -ray generation from the laser interaction in a carbon plasma channel,” *Frontiers in Physics* **10** (2022), 10.3389/fphy.2022.987830.
- [124] M Jirka, M Vranic, T Grismayer, and L O Silva, “Scaling laws for direct laser acceleration in a radiation-reaction dominated regime,” *New Journal of Physics* **22**, 083058 (2020).
- [125] R. F. Casten, “COLLECTIVE EXCITATIONS IN EVEN–EVEN NUCLEI: VIBRATIONAL AND ROTATIONAL MOTION,” (Oxford University Press Oxford, 2001) pp. 173–296.
- [126] C. J. Yang, K. M. Spohr, and D. Doria, “Multi-photon stimulated gratings assisted by laser-plasma interactions,” (2024), arXiv:2404.10025 [physics.optics].
- [127] Michael A. Purvis, Vyacheslav N. Shlyaptsev, Reed Hollinger, Clayton Bargsten, Alexander Pukhov, et al., “Relativistic plasma nanophotonics for ultrahigh energy density physics,” *Nature Photonics* **7**, 796–800 (2013).
- [128] Clayton Bargsten, Reed Hollinger, Maria Gabriela Capeluto, Vural Kaymak, Alexander Pukhov, et al., “Energy penetration into arrays of aligned nanowires irradiated with relativistic intensities: Scaling to terabar pressures,” *Science Advances* **3** (2017), 10.1126/sciadv.1601558.
- [129] Lihua Cao, Yuqiu Gu, Zongqing Zhao, Leifeng Cao, Wenzhong Huang, et al., “Enhanced absorption of intense short-pulse laser light by subwavelength nanolayered target,” *Physics of Plasmas* **17** (2010), 10.1063/1.3360298.
- [130] Zhanna Samsonova, Sebastian Höfer, Tino Kämpfer, Ingo Uschmann, Robert Röder, et al., “Hard x-ray generation from zno nanowire targets in a non-relativistic regime of laser-solid interactions,” *Applied Sciences* **8**, 1728 (2018).
- [131] G. Kulcsár, D. AlMawlawi, F. W. Budnik, P. R. Herman, M. Moskovits, et al., “Intense picosecond x-ray pulses from laser plasmas by use of nanostructured “velvet” targets,” *Physical Review Letters* **84**, 5149–5152 (2000).
- [132] G Cristoforetti, A Anzalone, F Baffigi, G Bussolino, G D’Arrigo, et al., “Investigation on laser–plasma coupling in intense, ultrashort irradiation of a nanostructured silicon target,” *Plasma Physics and Controlled Fusion* **56**, 095001 (2014).
- [133] Reed Hollinger, Clayton Bargsten, Vyacheslav N. Shlyaptsev, Vural Kaymak, Alexander Pukhov, et al., “Efficient picosecond x-ray pulse generation from plasmas in the radiation dominated regime,” *Optica* **4**, 1344 (2017).
- [134] K. A. Ivanov, D. A. Gozhev, S. P. Rodichkina, S. V. Makarov, S. S. Makarov, et al., “Nanostructured plasmas for enhanced gamma emission at relativistic laser interaction with solids,” *Applied Physics B* **123** (2017), 10.1007/s00340-017-6826-4.
- [135] Dimitri Khaghani, Mathieu Lobet, Björn Borm, Loïc Burr, Felix Gärtner, et al., “Enhancing laser-driven proton acceleration by using micro-pillar arrays at high drive energy,” *Scientific Reports* **7** (2017), 10.1038/s41598-017-11589-z.
- [136] L. A. Gizzi, G. Cristoforetti, F. Baffigi, F. Brandi, G. D’Arrigo, et al., “Intense proton acceleration in ultrarelativistic interaction with nanochannels,” *Physical Review Research* **2** (2020), 10.1103/physrevresearch.2.033451.
- [137] G Cristoforetti, F Baffigi, F Brandi, G D’Arrigo, A Fazzi, et al., “Laser-driven proton acceleration via excitation of surface plasmon polaritons into tio2 nanotube array targets,” *Plasma Physics and Controlled Fusion* **62**, 114001 (2020).
- [138] Deep Sarkar, Prashant Kumar Singh, G. Cristoforetti, Amitava Adak, Gourab Chatterjee, et al., “Silicon nanowire based high brightness, pulsed relativistic electron source,” *APL Photonics* **2** (2017), 10.1063/1.4984906.
- [139] A Moreau, R Hollinger, C Calvi, S Wang, Y Wang, et al., “Enhanced electron acceleration in aligned nanowire arrays irradiated at highly relativistic intensities,” *Plasma Physics and Controlled Fusion* **62**, 014013 (2019).
- [140] R. Hollinger, S. Wang, Y. Wang, A. Moreau, M. G. Capeluto, et al., “Extreme ionization of heavy atoms in solid-density plasmas by relativistic second-harmonic laser pulses,” *Nature Photonics* **14**, 607–611 (2020).
- [141] J. Park, R. Tommasini, R. Shepherd, R. A. London, C. Bargsten, et al., “Absolute laser energy absorption measurement of relativistic 0.7 ps laser pulses in nanowire arrays,” *Physics of Plasmas* **28** (2021), 10.1063/5.0035174.
- [142] X. Pan, M. Šmíd, L. G. Huang, T. Kluge, V. Bagnoud, et al., “Investigation on laser absorption and x-ray radiation in microstructured titanium targets heated by short-pulse relativistic laser pulses,” *Physical Review Research* **6** (2024), 10.1103/physrevresearch.6.013025.
- [143] Ya-Dong Xia, De-Feng Kong, Qiang-You He, Zhen Guo, Dong-Jun Zhang, et al., “Generation and regulation of electromagnetic pulses generated by femtosecond lasers interacting with multitargets,” *Nuclear Science and Techniques* **35** (2024), 10.1007/s41365-024-01381-w.
- [144] Yanlei Yang, Chong Lv, Wei Sun, Xiaona Ban, Qiushi Liu, et al., “Neutron generation enhanced by a femtosecond laser irradiating on multi-channel target,” *Frontiers in Physics* **11** (2023), 10.3389/fphy.2023.1189755.
- [145] Defeng Kong, Guoqiang Zhang, Yinren Shou, Shirui Xu, and Zhulong and others Mei, “High-energy-density plasma in femtosecond-laser-irradiated nanowire-array targets for nuclear reactions,” *Matter and Radiation at Extremes* **7** (2022), 10.1063/5.0120845.
- [146] Yue Chao, Lihua Cao, Chunyang Zheng, Zhanjun Liu,

- and Xiantu He, “Enhanced proton acceleration from laser interaction with a tailored nanowire target,” *Applied Sciences* **12**, 1153 (2022).
- [147] B. Arad, S. Eliezer, and Y. Paiss, “Nuclear “anti-stokes” transitions induced by laser radiation,” *Physics Letters A* **74**, 395–397 (1979).
- [148] W. Becker, R.R. Schlicher, and M.O. Scully, “Laser-induced nuclear anti-stokes transitions revisited,” *Physics Letters A* **106**, 441–445 (1984).
- [149] Robert A. Müller, Andrey V. Volotka, and Andrey Surzhykov, “Excitation of the ^{229}Th nucleus via a two-photon electronic transition,” *Phys. Rev. A* **99**, 042517 (2019).
- [150] BS Ishkhanov and IM Piskarev, “Excitation of γ -laser using the nuclear raman effect,” *Yadernaya Fizika* **32**, 593–594 (1980).
- [151] E V Baklanov and V P Chebotaev, “Possible development of a γ -ray laser,” *Soviet Journal of Quantum Electronics* **6**, 345–347 (1976).
- [152] F. Winterberg, “Beating the graser dilemma by rapid heat-removal under high pressure,” *AIP Conference Proceedings* (1986), 10.1063/1.35822.
- [153] S Eliezer, JM Martinez-Val, Y Paiss, and G Velarde, “Induced stokes or anti-stokes nuclear transitions,” *Quantum Electronics* **25**, 1106 (1995).
- [154] S Eliezer, JM Martinezval, and JL Borowitz, “On the possibility for a gamma-ray laser,” *Laser Physics* **5**, 323–325 (1995).
- [155] Lev A Rivlin, “Two-quantum-induced energy release of isomeric nuclei,” *Quantum Electronics* **34**, 23–28 (2004).
- [156] T. Tajima and J. M. Dawson, “Laser electron accelerator,” *Phys. Rev. Lett.* **43**, 267–270 (1979).
- [157] E. Esarey, C. B. Schroeder, and W. P. Leemans, “Physics of laser-driven plasma-based electron accelerators,” *Rev. Mod. Phys.* **81**, 1229–1285 (2009).
- [158] Félicie Albert and Alec G R Thomas, “Applications of laser wakefield accelerator-based light sources,” *Plasma Physics and Controlled Fusion* **58**, 103001 (2016).
- [159] Donna Strickland and Gerard Mourou, “Compression of amplified chirped optical pulses,” *Optics Communications* **55**, 447–449 (1985).